ChemComm

Central metal dependent modulation of induced-fit gas uptake in molecular porphyrin solids

Journal:	*ChemComm*
Manuscript ID	CC-COM-05-2018-003646.R2
Article Type:	Communication

Chemical Communications

COMMUNICATION

Central metal dependent modulation of induced-fit gas uptake in molecular porphyrin solids†

Received 00th January 20xx,
Accepted 00th January 20xx

DOI: 10.1039/x0xx00000x

www.rsc.org/

Hirotomo Nishihara,*[a] Mao Ohwada,[a] Takuya Kamimura,[b] Masato Nishimura,[b] Hideki Tanaka,[c] Shotaro Hiraide,[c] Minoru T. Miyahara,[c] Katsuhiko Ariga,[d,e] Qingmin Ji,[d,f] Jun Maruyama,[g] and Fumito Tani*[c]

Induced-fit accommodation of a variety of gaseous molecules including non-polar molecules has been demonstrated in porphyrin-based supramolecular architectures for the first time. Moreover, the gas uptake behaviour can be modulated by the central cation of porphyrin.

A great deal of attention has been paid to advanced porous frameworks such as metal-organic frameworks (MOFs),[1, 2] porous organic polymers (POPs),[3, 4] and hydrogen-bonded frameworks (HBFs).[5] These materials can be designed and synthesized by the methodologies of organic and/or coordination chemistry, unlike conventional disordered porous materials, such as porous carbons and porous silicas. Among a variety of building units, porphyrin has fascinating advantages of chemical/thermal stability, robust nature, facile synthesis, and ubiquitous biological functions such as light-harvesting, oxygen transportation, and catalysis.[6, 7] Thus, porphyrin-based porous frameworks which possess gas-accessible permanent porosities have been intensively developed as the forms of MOFs,[8-16] POPs,[17-20] and HBFs.[21, 22]

On the other hand, organic solids composed by van der Waals forces are also expected as another type of gas-sorptive materials. There are two mechanisms for gas uptake: (1) physisorption in permanent nanospaces at inter-molecular spaces and/or internal nanospaces existing inside cage-shaped[23, 24] or ring-shaped[25] molecules, and (2) accommodating guests by the rearrangement of molecular orientation, called 'induced-fit' accommodation.[26, 27] In (2), even non-porous solids can accommodate gas molecules, and moreover, complex gas uptake behaviour by hybrid mechanism of (1) and (2) has been also reported.[28-30] These sorptive van der Waals solids (SVSs) have potential advantages, such as solution processability, applicability of 'mix and match' strategy, and a high guest-responsiveness, compared to framework-based porous materials.[24, 31] Thus, porphyrin-based porous cage molecules have been also reported recently.[32] On the other hand, induced-fit gas uptake in porphyrin-based SVSs has not been reported, while it has been possible in solution[33]. Herein, we demonstrate it in porphyrin-based SVSs, cyclic porphyrin dimers (CPDs),[34, 35] and moreover, the on-off porosity switching can be modulated simply by changing the central cation of CPDs.

As shown in Fig. 1a, CPD bearing diacetylene linkers and 4-pyridyl groups is used as a basic molecular framework in this work. Figs. 1b and 1c show the crystal structures of free base (M = 2H; **1a**)[35] and Ni(II)-metalated (M = Ni; **2a**)[34] CPDs, accommodating *o*-dichlorobenzene and toluene inside the CPD rings, respectively. Four pyridyl groups on the side edges of the porphyrin planes weakly interact with each other, and CPDs form a self-assembled nanotube structure shown in Figs. 1b and 1c. Thus, CPDs possess the ability of forming guest-accommodating structures by crystallisation from solution. This work aims to study gas uptake, and therefore, guest-free forms of **1a** and **2a** were prepared by using easily removable chloroform as the final solvent for their synthesis. The obtained solids are denoted as **1b** and **2b**, respectively. Absence of guest molecules was confirmed by ^{1}H-NMR (Fig. S1†) and thermogravimetry (Fig. S2†). As is found from very small adsorption amounts of CO_2 at 298 K in **1b** and **2b** (Fig. 1d), these guest-free forms are densely-packed solids without noticeable permanent porosity. Fig. S3† shows the powder X-ray diffraction (PXRD) patterns of **1a**, **1b**, **2a**, and **2b**. **1b** displays a few intense and sharp peaks, along with broad and weak peaks, indicating that the CPD packing structure includes

[a] Institute of Multidisciplinary Research for Advanced Materials, Tohoku University, 2-1-1, Katahira, Aoba-ku, Sendai, 980-8577, Japan.
[b] Institute for Materials Chemistry and Engineering, Kyushu University, 744 Motooka, Nishi-ku, Fukuoka 819-0395, Japan
[c] Department of Chemical Engineering, Kyoto University, Katsura, Nishikyo, Kyoto 615-8510, Japan
[d] World Premier International (WPI) Research Center for Materials, Nanoarchitechtonics (MANA), National Institute for Materials Science (NIMS), 1-1 Namiki, Tsukuba, Ibaraki 305-0044, Japan
[e] Department of Advanced Materials Science, Graduate School of Frontier Sciences, The University of Tokyo, 5-1-5 Kashiwanoha, Kashiwa, Chiba 277-8561, Japan
[f] Nanjing University of Science and Technology, 200 Xiaolingwei, Jiangsu, 210094, China
[g] Research Division of Environmental Technology, Osaka Research Institute of Industrial Science and Technology, 1-6-50, Morinomiya, Joto-ku, Osaka 536-8553, Japan
hirotomo.nishihara.b1@tohoku.ac.jp; tanif@ms.ifoc.kyushu-u.ac.jp
† Electronic Supplementary Information (ESI) available: See
DOI: 10.1039/x0xx00000x

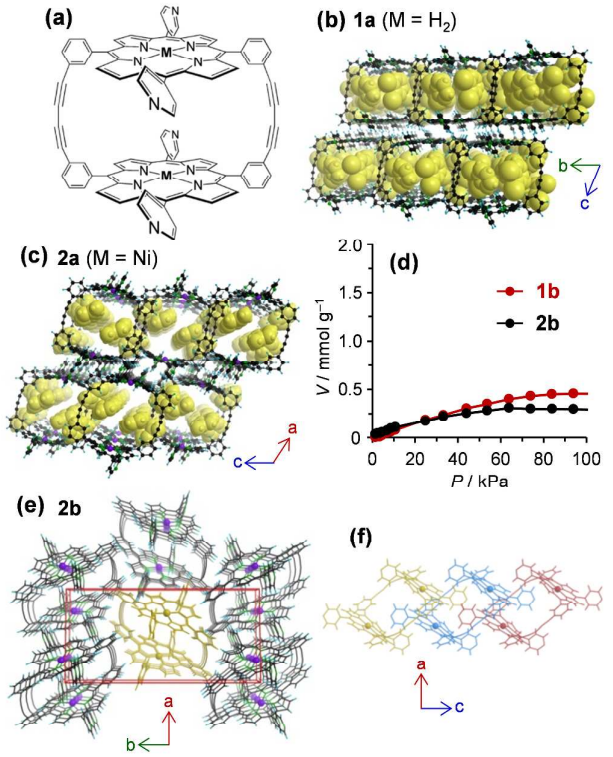

Fig. 1 (a) Chemical structure of M_2-CPD (M = H_2 or Ni). (b,c) Crystal structures of (b) **1a** (M = H_2; CCDC-780017; CDC-VAGKAR) and (c) **2a** (M = Ni; CCDC-658588; CDC-MIWYUN) accommodating guest (solvent) molecules which are shown by yellow space-filling models. (d) CO_2 adsorption isotherms on **1b** and **2b**, measured at 298 K. (e) The crystal packing of **2b** viewed from the <100> direction (CCDC-1552441; CDC-KAYCAR). A red lattice is the unit cell. A columnar array of CPD molecules is highlighted by yellow colour. In (b), (c), and (e), C, H, N, O, Ni = black, light blue, green, red, and purple, respectively. (f) The columnar array of **2b** molecules viewed from the <010> direction; each molecule is displayed in a different colour.

some disorder. Thus, it is not possible to determine the exact crystal structure of **1b**. On the other hand, **2b** is a well-crystalline solid with the densely packing structure as shown in Fig. 1e.[36] The inside space of a CPD molecule is occupied by pyridine groups of the neighboring molecules (Fig. 1f), and thus, **2b** does not possess permanent porosity. The predominant intermolecular interactions are weak van der Waals forces in **1b** and **2b**, and it is expected that gas molecules may trigger the rearrangement of CPD orientation through the induced-fit mechanism, especially in **1b** which has the looser packing structure.

Thus, we have examined adsorption isotherms of a variety of gases on **1b** and **2b** (Fig. 2). Non-logarithmic diagrams for Figs. 2a-c are shown in Fig. S4†. As for N_2 adsorption at 77K (Fig. 2a), the same measurement was repeated twice. At the first measurement, **1b** shows a specific adsorption isotherm in which sudden gas uptake occurs at P/P_0 = 0.01-0.03, and a desorption branch does not overlap the adsorption. The second isotherms agree well with the first results, indicating that the specific gas uptake is reversible without irreversible permanent structure change/destruction. These are the typical behaviour at the induced-fit gas accommodation.[28, 37] Indeed, the change of the **1b** packing structure was confirmed by *in situ* PXRD measurement as shown later. On the other hand, **2b** accommodates a smaller amount of N_2 at P/P_0 near 1, and the desorption isotherm is not closed, also showing the behaviour of the induced-fit gas accommodation, although the uptake pressure and the amount are very different from those of **1b**. Thus, the difference of the central cation can significantly change the gas uptake property. The results for Ar at 87 K (Fig. 2b) are basically similar to those of N_2 at 77 K (Fig. 2a). The different gas-uptake properties in **1b** and **2b** can be ascribed to their different molecular packings depending on the central cations. In **2b**, CPD molecules are closely packed (Figs. 1e and 1f), and each CPD molecule more hardly moves against the stimulus by N_2 or Ar, whereas the CPD molecules in 1b can

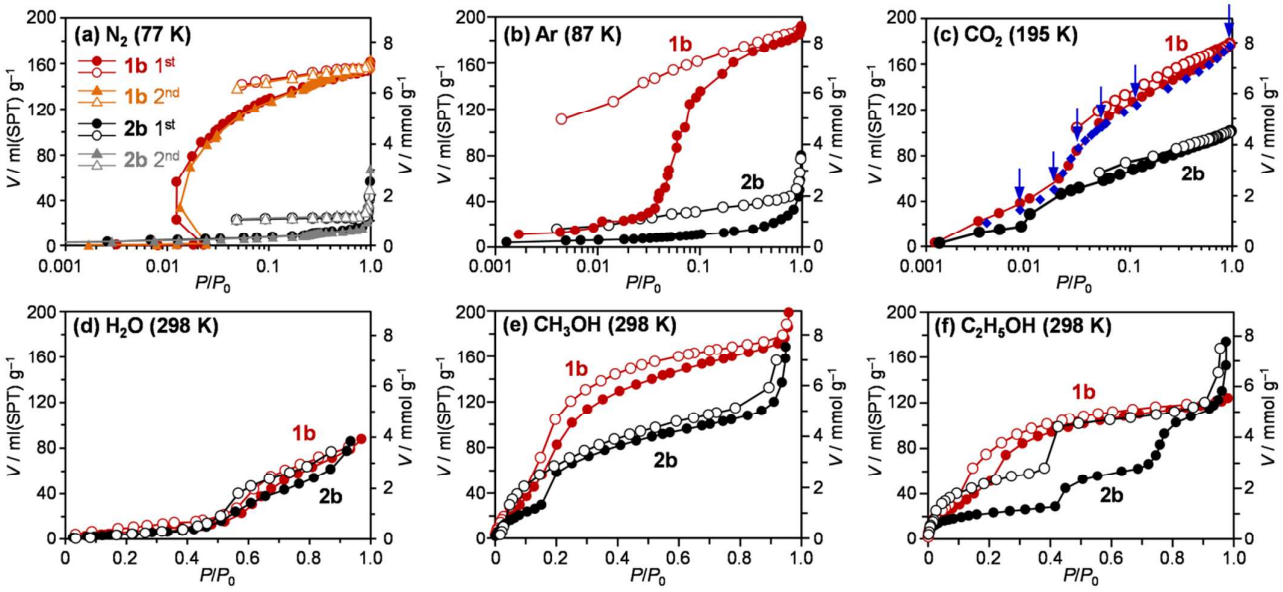

Fig. 2 Adsorption-desorption isotherms of a variety of gases on **1b** and **2b**. Adsorption and desorption data are shown by solid and blank markers, respectively. (a) N_2 at 77 K. The measurements were repeated twice, and all the results are shown together. (b) Ar at 87 K. (c) CO_2 at 195 K. For **1b**, the adsorption isotherm measured for *in situ* PXRD is shown by solid diamond. The PXRD patterns at the arrowed data points are shown in Fig. 3a. (d) H_2O at 298 K. (e) Methanol at 298 K. (f) Ethanol at 298 K. P/P_0 is shown by a logarithm scale in (a-c) for better views of induced-fit uptakes.

easily move because of their relatively loose packing.

Fig. 2c shows the CO_2 adsorption-desorption isotherms at 195 K, and **1b** exhibits the induced-fit behaviour. Unlike at 298 K, lower temperature is favour for physisorption and it is thus found that the temperature is also an important factor for the induced-fit accommodation. To confirm the structure change of **1b** upon the CO_2 uptake, *in situ* PXRD analysis was carried out at the several data points highlighted in Fig. 2c. The results are shown in Fig. 3a. At the pressure range below P/P_0 = 0.018, **1b** gradually accommodates CO_2 up to 2.24 mmol g^{-1} (Fig. 2c), corresponding to ca. 3 mol mol^{-1} (3 CO_2 molecules per one CPD molecule; Fig. S5†). During this period, the peaks of the PXRD patterns become weak as well as broaden, and their positions are shifted to lower angle, indicating gradual disordering of the CPD arrangement together with expansion of the packing structure. The *d*-spacing calculated from the most intense peak (Fig. 3a, inset) is increased from 1.41 nm (P/P_0 = 0) to 1.44 nm (P/P_0 = 0.018). Such structure change slightly generates inter-molecular spaces into which CO_2 can invade. At P/P_0 between 0.018 and 0.031, a rapid uptake occurs up to ca. 5 mol mol^{-1}, and the PXRD pattern shows a drastic change (Fig. 3a). Thus, it is confirmed that the rearrangement of CPD molecules occurs by the induced-fit accommodation. Above P/P_0 = 0.031, **1b** gradually uptakes CO_2 molecules up to 10–11 mol mol^{-1}, and PXRD peaks gradually become sharper and more intense without significant shift of their positions. The *d*-spacing calculated from the most intense peak (Fig. 3a, inset) is only slightly increased from 1.48 nm (P/P_0 = 0.031) to 1.49 nm (P/P_0 = 0.95). The above results indicate that most of **1b** transforms into a new porous phase capable to include guest molecules at once around P/P_0 = 0.031. At this moment, the new crystal does not fully accommodate guest molecules and the domain size is relatively small. At higher P/P_0, the new crystal gradually adsorbs guest molecules, and the crystal domains grow larger. The CO_2 uptake amount in **1b** at 195 K was then compared to that in a hypothetical guest-free framework of **1a**. The latter was calculated by the Grand Canonical Monte Carlo (GCMC) simulation[38] (Fig. S6†). The results indicate that the framework porosity of the new crystalline phase of **1b** accommodating CO_2 is about the half of that of **1a**.

In Fig. 2c, **2b** shows large CO_2 uptake compared to those of N_2 (Fig. 2a) and Ar (Fig. 2b), probably due to the larger quadruple moment of CO_2 (4.30×10^{26} esu cm^2) than those of N_2 (1.52×10^{26} esu cm^2) and Ar (0 esu cm^2).[39] Thus, the stronger the interaction between adsorbent and adsorptive becomes, the easier the induced-fit rearrangement becomes.

Figs. 2d-f show gas (vapor) adsorption-desorption isotherms of H_2O (2d), methanol (2e), and ethanol (2f) on **1b** and **2b**. While **1b** and **2b** exhibit very similar uptake behaviour to H_2O, their behaviours greatly differ as for methanol and ethanol. Interestingly, **2b** shows unique multi-step uptakes for methanol (3 steps) and ethanol (4 steps). Such specific phase transition may be useful to gas sensor applications. BET surface areas (S_{BET}) and total pore volumes (V_{total}) calculated from the isotherms shown in Fig. 2 are summarized in Table S1† for reference. **1b** and **2b** exhibits different uptake behaviours depending on the guest gases. While **1b** shows a largest uptake for CO_2 (195 K) with V_{total} = 0.34 cm^3 g^{-1}, **2b** shows a largest uptake for ethanol (298 K) with V_{total} = 0.31 cm^3 g^{-1}.

The crystalline structures of **1b** and **2b** upon accommodating gas molecules are analysed by PXRD as shown in Figs 3b and c. For **1b**, the inclusion crystal structures can be roughly classified into three groups: (1) N_2 and CO_2, (2) H_2O, methanol, and ethanol, and (3) *o*-dichlorobenzene (**1a**). Also for **2b**, it is found from Fig. 3c that inclusion of H_2O, methanol, or ethanol forms the similar crystalline phase which is different

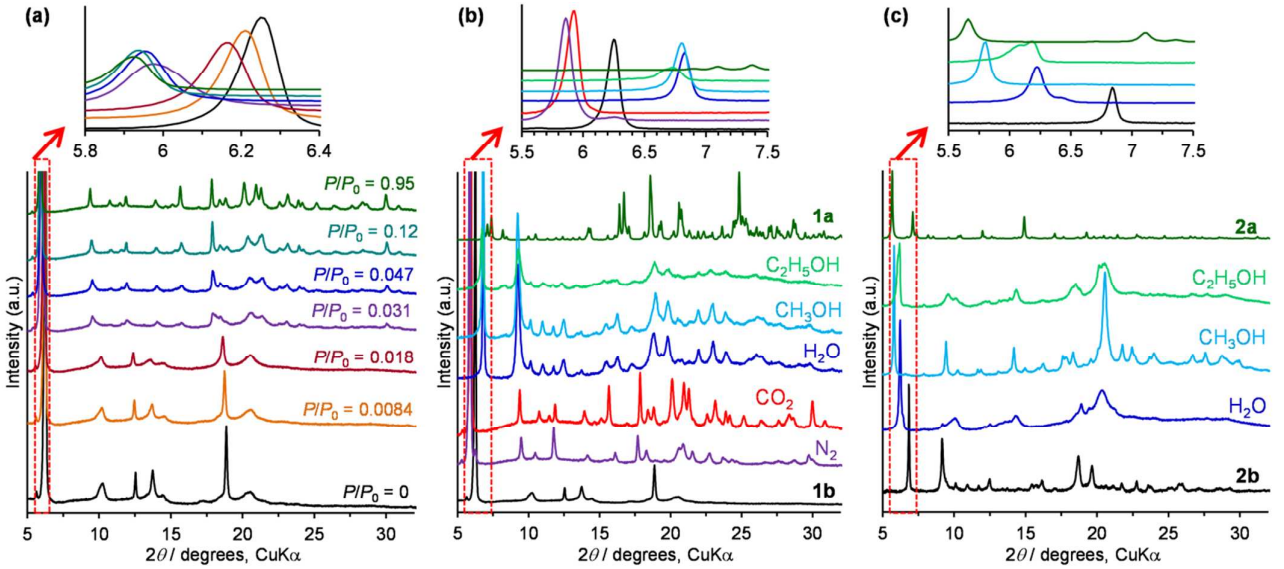

Fig. 3 (a) *In situ* PXRD patterns of **1b** during the CO_2 adsorption measurement (the isotherm data are shown in Fig. 2c). Each pattern was obtained when the adsorption achieved equilibrium at the corresponding P/P_0. (b,c) PXRD patterns of (b) **1b** and (c) **2b** with and without inclusion of a variety of molecules. The patterns of **1b** accommodating N_2 and CO_2 were obtained at P/P_0 = 0.95 by the same manner for (a). The patterns of **1b** and **2b** accommodating H_2O, CH_3OH, and C_2H_5OH were obtained by synchrotron X-ray irradiated on the samples which were achieved to adsorption equilibrium under P/P_0 = 1 and encapsulated in a closed glass capitally. The data labelled **1a** and **2a** are simulated patterns from the crystal structures accommodating *o*-dichlorobenzene and toluene, respectively. Insets show enlarged patterns at the highlighted areas.

from the one formed by toluene (**2a**). Thus, CPD molecules has an ability of forming several different inclusion crystals depending on the host molecules, and the induced-fit behaviour can be greatly modulated simply by changing the porphyrin central cations. A gas uptake ability of **1b** was further examined by a variety of gases, and found that the gas uptake behaviour greatly varies depending on the type of gases (Fig. S7[†]). Thus, this work demonstrates an interesting possibility of porphyrin-based SVSs towards versatile applications based on the selective gas uptake ability of CPDs.

In summary, induced-fit gas uptake has been demonstrated in porphyrin-based sorptive van der Waals solids (SVSs), cyclic porphyrin dimers (CPDs). Depending on the central cations of CPDs, the induced-fit behaviour can be remarkably modulated. This means that it is possible to tune the selectivity of gas uptake even by very minor change of the host molecular structure. From the tunable selectivity of gases and the versatile function of porphyrin moiety, porphyrin-based SVSs are expected as new class of gas sorptive materials.

This work is supported by JST PREST network; the Dynamic Alliance for Open Innovation Bridging Human, Environment and Materials; and the Network Joint Research Centre for Materials and Devices. A part of PXRD measurements was performed in SPring-8 (Proposals no. 2015A1956, 2016B1874).

Conflicts of interest

There are no conflicts to declare.

Notes and references

1 S. Kitagawa, R. Kitaura and S. Noro, *Angew. Chem. Int. Ed.*, 2004, **43**, 2334-2375.
2 H. Furukawa, K. E. Cordova, M. O'Keeffe and O. M. Yaghi, *Science*, 2013, **341**, 974-986.
3 A. Thomas, *Angew. Chem. Int. Ed.*, 2010, **49**, 8328-8344.
4 Z. Xiang and D. Cao, *J. Mater. Chem. A*, 2013, **1**, 2691-2718.
5 T. Adachi and M. D. Ward, *Acc. Chem. Res.*, 2016, **49**, 2669-2679.
6 M. E. Kosal and K. S. Suslick, *J. Solid State Chem.*, 2000, **152**, 87-98.
7 W. Y. Gao, M. Chrzanowski and S. Q. Ma, *Chem. Soc. Rev.*, 2014, **43**, 5841-5866.
8 D. W. Smithenry, S. R. Wilson and K. S. Suslick, *Inorg. Chem.*, 2003, **42**, 7719-7721.
9 T. Ohmura, A. Usuki, K. Fukumori, T. Ohta, M. Ito and K. Tatsumi, *Inorg. Chem.*, 2006, **45**, 7988-7990.
10 K. Sato, *Transactions of the Materials Research Society of Japan*, 2010, **35**, 515-517.
11 O. K. Farha, A. M. Shultz, A. A. Sarjeant, S. T. Nguyen and J. T. Hupp, *J. Am. Chem. Soc.*, 2011, **133**, 5652-5655.
12 C. Y. Lee, O. K. Farha, B. J. Hong, A. A. Sarjeant, S. T. Nguyen and J. T. Hupp, *J. Am. Chem. Soc.*, 2011, **133**, 15858-15861.
13 H.-L. Jiang, D. Feng, K. Wang, Z.-Y. Gu, Z. Wei, Y.-P. Chen, et al., *J. Am. Chem. Soc.*, 2013, **135**, 13934-13938.
14 Y. Y. Liu, Y. M. Yang, Q. L. Sun, Z. Y. Wang, B. B. Huang, Y. Dai, et al., *ACS Appl. Mater. Interfaces*, 2013, **5**, 7654-7658.
15 K. Wang, X.-L. Lv, D. Feng, J. Li, S. Chen, J. Sun, et al., *J. Am. Chem. Soc.*, 2016, **138**, 914-919.
16 X.-L. Lv, K. Wang, B. Wang, J. Su, X. Zou, Y. Xie, et al., *J. Am. Chem. Soc.*, 2017, **139**, 211-217.
17 N. B. McKeown, S. Hanif, K. Msayib, C. E. Tattershall and P. M. Budd, *Chem. Commun.*, 2002, 2782-2783.
18 A. Modak, M. Nandi, J. Mondal and A. Bhaumik, *Chem. Commun.*, 2012, **48**, 248-250.
19 Z. Wang, S. Yuan, A. Mason, B. Reprogle, D.-J. Liu and L. Yu, *Macromolecules*, 2012, **45**, 7413-7419.
20 X. S. Wang, J. Liu, J. M. Bonefont, D. Q. Yuan, P. K. Thallapally and S. Q. Ma, *Chem. Commun.*, 2013, **49**, 1533-1535.
21 K. Ariga, K. Endo, Y. Aoyama and Y. Okahata, *Colloid. Surf. A*, 2000, **169**, 177-186.
22 Z. Q. Zhang, J. Li, Y. H. Yao and S. Sun, *Cryst. Growth Des.*, 2015, **15**, 5028-5033.
23 J. L. Atwood, L. J. Barbour and A. Jerga, *Science*, 2002, **296**, 2367-2369.
24 T. Tozawa, J. T. A. Jones, S. I. Swamy, S. Jiang, D. J. Adams, S. Shakespeare, et al., *Nat. Mater.*, 2009, **8**, 973-978.
25 T. Ogoshi, R. Sueto, K. Yoshikoshi and T.-a. Yamagishi, *Chem. Commun.*, 2014, **50**, 15209-15211.
26 J. L. Atwood, L. J. Barbour, A. Jerga and B. L. Schottel, *Science*, 2002, **298**, 1000-1002.
27 P. K. Thallapally, B. P. McGrail, S. J. Dalgarno, H. T. Schaef, J. Tian and J. L. Atwood, *Nat Mater*, 2008, **7**, 146-150.
28 T. Mitra, X. Wu, R. Clowes, J. T. Jones, K. E. Jelfs, D. J. Adams, et al., *Chem.-Eur. J.*, 2011, **17**, 10235-10240.
29 T. Hasell, J. L. Culshaw, S. Y. Chong, M. Schmidtmann, M. A. Little, K. E. Jelfs, et al., *J. Am. Chem. Soc.*, 2014, **136**, 1438-1448.
30 M. A. Little, S. Y. Chong, M. Schmidtmann, T. Hasell and A. I. Cooper, *Chem. Commun.*, 2014, **50**, 9465-9468.
31 J. T. Jones, T. Hasell, X. Wu, J. Bacsa, K. E. Jelfs, M. Schmidtmann, et al., *Nature*, 2011, **474**, 367-371.
32 S. Hong, M. R. Rohman, J. Jia, Y. Kim, D. Moon, Y. Kim, et al., *Angew. Chem. Int. Ed.*, 2015, **54**, 13241-13244.
33 B. C. Deutman Alexander, M. M. Smits Jan, R. de Gelder, A. A. W. Elemans Johannes, J. M. Nolte Roeland and E. Rowan Alan, *Chem.-Eur. J.*, 2014, **20**, 11574-11583.
34 H. Nobukuni, Y. Shimazaki, F. Tani and Y. Naruta, *Angew. Chem. Int. Ed.*, 2007, **46**, 8975-8978.
35 H. Nobukuni, Y. Shimazaki, H. Uno, Y. Naruta, K. Ohkubo, T. Kojima, et al., *Chem.-Eur. J.*, 2010, **16**, 11611-11623.
36 H. Nishihara, T. Hirota, K. Matsuura, M. Ohwada, N. Hoshino, T. Akutagawa, et al., *Nat. Commun.*, 2017, **8**, 109.
37 S. Horike, S. Shimomura and S. Kitagawa, *Nat, Chem.*, 2009, **1**, 695.
38 H. Nishihara, H. Fujimoto, H. Itoi, K. Nomura, H. Tanaka, M. T. Miyahara, et al., *Carbon*, 2018, **129**, 854-862.
39 J.-R. Li, R. J. Kuppler and H.-C. Zhou, *Chem. Soc. Rev.*, 2009, **38**, 1477-1504.

Table of contents entry

Textual abstract

Induced-fit gas uptake in supramolecular sorbent materials has attracted great interest from its potential for versatile applications which cannot be achieved by classical physisorption in porous solids. In this work, we report the induced-fit gas uptake in porphyrin-based supramolecular architecture, and moreover, the on-off porosity switching can be modulated simply by changing the central cation of porphyrin.

Graphical abstract